INTERNATIONAL JOURNAL FOR NUMERICAL METHODS IN ENGINEERING, VOL. 28, 1449–1460 (1989)

DEVELOPMENT AND APPLICATIONS OF TWO SINGULAR POINTS FINITE ELEMENTS

B. K. DUTTA

Reactor Engineering Division, Bhabha Atomic Research Centre, Bombay-85, India

S. K. MAITI

Department of Mechanical Engineering, Indian Institute of Technology, Powai, Bombay 400076, India

A. KAKODKAR

Reactor Engineering Division, Bhabha Atomic Research Centre, Bombay-85, India

SUMMARY

An element formulation is suggested to obtain variable order singularities simultaneously at the two neighbouring corner nodes of a 4-noded quadrilateral. The element is useful for modelling a kinked crack with small kink length. The accuracy is good and this is obtained at a substantially reduced computational cost. Case studies are presented to illustrate the usefulness and the accuracy obtainable.

INTRODUCTION

Under mixed mode loading a crack leads to an out-of-plane extension and hence kinking. In stable crack propagation studies under this type of loading, one has to deal with kinked cracks. For a small kink length, an analysis of the problem is difficult owing to the existence of two singular points at a close distance. At the crack tip, there is a square root singularity, whereas at the knee the order of singularity depends on the kink angle.[1] One obvious strategy is to use the well-known quarter point elements[2] at the crack tip for the simulation of square root singularity and the 3-noded variable order triangular singularity elements[3] at the knee. The two elements must be separated by a number of conventional elements. This will usually lead to a large number of elements and nodes and hence more computational cost. One alternative strategy is to use one single element to cover the whole kink length. This would therefore require an element with two variable order singularities at the two neighbouring corner nodes.

In the following we present a formulation to generate such an element with four nodes. The element is called a two singular points (TSP) element. An adoption of this element in a displacement based finite element computer code is quite easy. The element has been used first to study a kinked crack problem analysed by earlier investigators.[3] It is then used to examine a kinked crack with different kink angles. In this case J's are computed and compared with analytical results based on the first order approximate method of Cotterell and Rice[4] and those due to finite element computation by Sethuraman and Maiti.[5] The effect of mesh refinement on computation of J and the path independence of J are examined in this case. A third case study is presented to show the range of kink sizes with respect to the main crack that can be modelled by the TSP element.

0029–5981/89/061449–12$06.00

Received 13 October 1987
Revised 2 August 1988

ELEMENT FORMULATION

Consider a 4-noded quadrilateral element as shown in Figure 1(a). The element can be mapped into a square in the conventional (ξ, η) system of natural co-ordinates (Figure 1(b)). Consider now a local co-ordinate system (ρ_1, ρ_2) defined by

$$\rho_1 = (2+\xi+\eta)/4 \quad \text{and} \quad \rho_2 = (2-\xi+\eta)/4 \tag{1}$$

In this (ρ_1, ρ_2) system the co-ordinates of the four corner nodes are shown in Figure 1(b). The equations of the four sides of the element are

$$\begin{aligned} L_{12} &= \rho_1 + \rho_2 - 0{\cdot}5 = 0, && \text{for side 1–2} \\ L_{23} &= -\rho_1 + \rho_2 + 0{\cdot}5 = 0, && \text{for side 2–3} \\ L_{34} &= \rho_1 + \rho_2 - 1{\cdot}5 = 0, && \text{for side 3–4} \end{aligned} \tag{2}$$

and

$$L_{41} = -\rho_1 + \rho_2 - 0{\cdot}5 = 0, \quad \text{for side 4–1}$$

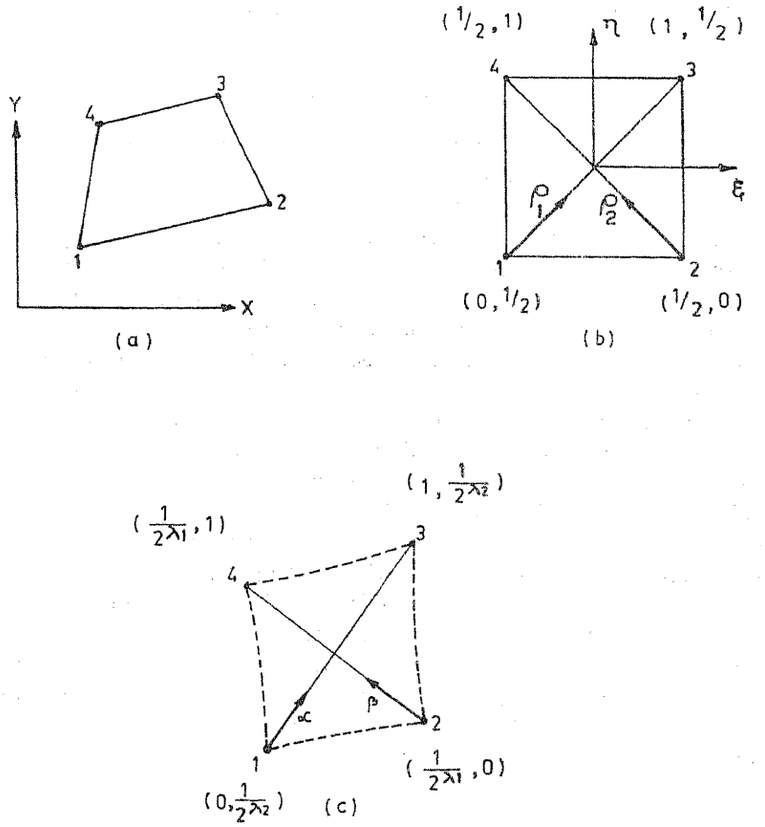

Figure 1. Illustration used to derive the displacement shape functions for a TSP element

The conventional shape functions associated with the four corner nodes can be written as

$$\begin{aligned} N_1 &= -(-\rho_1+\rho_2+0{\cdot}5)(\rho_1+\rho_2-1{\cdot}5) = C_1 L_{23} L_{34} \\ N_2 &= (\rho_1+\rho_2-1{\cdot}5)(-\rho_1+\rho_2-0{\cdot}5) = C_2 L_{34} L_{41} \\ N_3 &= -(-\rho_1+\rho_2-0{\cdot}5)(\rho_1+\rho_2-0{\cdot}5) = C_3 L_{41} L_{12} \end{aligned} \tag{3}$$

and

$$N_4 = (\rho_1+\rho_2-0{\cdot}5)(-\rho_1+\rho_2+0{\cdot}5) = C_4 L_{12} L_{23}$$

Note that $C_1 = C_3 = -1$ and $C_2 = C_4 = 1$. These are obtained from the fact that N_i is 1 at node i, $i = 1, 2, 3$ and 4. Consider a mapping $\alpha = \rho_1^{\lambda_1}$ and $\beta = \rho_2^{\lambda_2}$. α and β form an orthogonal system of co-ordinates. The element in the (α, β) system is shown in Figure 1(c). The equation of the four straight lines joining the nodes is

$$\begin{aligned} L_{ij} &= A_{ij}\alpha + \beta + B_{ij} \\ &= A_{ij}\rho_1^{\lambda_1} + \rho_2^{\lambda_2} + B_{ij} \end{aligned} \tag{4}$$

where A_{ij} and B_{ij} are constants. Four shape functions can be then constructed using (3). C_i is adjusted such that N_i is unity at node i. These shape functions are given below explicitly.

$$\begin{aligned} N_1 &= C_1(A_{23}\rho_1^{\lambda_1} + \rho_2^{\lambda_2} + B_{23})(A_{34}\rho_1^{\lambda_1} + \rho_2^{\lambda_2} + B_{34}) \\ N_2 &= C_2(A_{34}\rho_1^{\lambda_1} + \rho_2^{\lambda_2} + B_{34})(A_{41}\rho_1^{\lambda_1} + \rho_2^{\lambda_2} + B_{41}) \\ N_3 &= C_3(A_{41}\rho_1^{\lambda_1} + \rho_2^{\lambda_2} + B_{41})(A_{12}\rho_1^{\lambda_1} + \rho_2^{\lambda_2} + B_{12}) \end{aligned} \tag{5}$$

and

$$N_4 = C_4(A_{12}\rho_1^{\lambda_1} + \rho_2^{\lambda_2} + B_{12})(A_{23}\rho_1^{\lambda_1} + \rho_2^{\lambda_2} + B_{23})$$

where

$$\begin{aligned} A_{12} &= 2^{\lambda_1}/2^{\lambda_2} \\ B_{12} &= -1/2^{\lambda_2} \\ C_1 &= [2^{2\lambda_2}(1-2^{\lambda_1})^2]/[2^{2\lambda_1}(1-2^{\lambda_2})] \\ A_{23} &= 2^{\lambda_1}/[2^{\lambda_2}(1-2^{\lambda_1})] \\ B_{23} &= 1/[2^{\lambda_2}(2^{\lambda_1}-1)] \\ C_2 &= 1 \\ A_{34} &= [2^{\lambda_1}(1-2^{\lambda_2})]/[2^{\lambda_2}(1-2^{\lambda_1})] \\ B_{34} &= [2^{\lambda_1}(2^{\lambda_2}-1)]/[2^{\lambda_2}(1-2^{\lambda_1})] - 1/2^{\lambda_2} \\ C_3 &= 2^{2\lambda_2}/[2^{2\lambda_1}(1-2^{\lambda_2})] \\ A_{41} &= 2^{\lambda_1}(1-2^{\lambda_2})/2^{\lambda_2} \\ B_{41} &= -1/2^{\lambda_2} \end{aligned} \tag{6}$$

and

$$C_4 = 1$$

If the displacement field is written using these shape functions, i.e. $u = \sum_1^4 N_i u_i$ and $v = \sum_1^4 N_i v_i$, an element is obtained which displays strain/stress singularities at the corners 1 and 2. The orders of singularity are $-1+\lambda_1$ and $-1+\lambda_2$. The element meets the completeness requirement,

i.e. $\sum_{1}^{4} N_i = 1$, only when $\lambda_1 = \lambda_2 = 1$. The derivatives of the shape functions with respect to (ξ, η) are given by

$$\partial N_i/\partial \xi = \partial N_i/\partial \rho_1 \, \partial \rho_1/\partial \xi + \partial N_i/\partial \rho_2 \, \partial \rho_2/\partial \xi$$

and

$$\partial N_i/\partial \eta = \partial N_i/\partial \rho_1 \, \partial \rho_1/\partial \eta + \partial N_i/\partial \rho_2 \, \partial \rho_2/\partial \eta$$

Using $\partial \rho_1/\partial \xi = 0{\cdot}25$, $\partial \rho_2/\partial \xi = -0{\cdot}25$, $\partial \rho_1/\partial \eta = 0{\cdot}25$ and $\partial \rho_2/\partial \eta = 0{\cdot}25$ these derivatives can be written finally in the following form.

$$\begin{aligned}
\partial N_1/\partial \xi &= C_1[\lambda_1 \rho_1^{\lambda_1 - 1}[2A_{23}A_{34}\rho_1^{\lambda_1} + (A_{23} + A_{34})\rho_2^{\lambda_2} \\
&\quad + (A_{23}B_{34} + A_{34}B_{23})] - \lambda_2 \rho_2^{\lambda_2 - 1}[(A_{34} + A_{23})\rho_1^{\lambda_1} \\
&\quad + 2\rho_2^{\lambda_2} + (B_{34} + B_{23})]]/4 \\
\partial N_1/\partial \eta &= C_1[\lambda_1 \rho_1^{\lambda_1 - 1}[2A_{23}A_{34}\rho_1^{\lambda_1} + (A_{23} + A_{34})\rho_2^{\lambda_2} \\
&\quad + (A_{23}B_{34} + A_{34}B_{23})] + \lambda_2 \rho_2^{\lambda_2 - 1}[(A_{34} + A_{23})\rho_1^{\lambda_1} \\
&\quad + 2\rho_2^{\lambda_2} + (B_{34} + B_{23})]]/4 \\
\partial N_2/\partial \xi &= C_2[\lambda_1 \rho_1^{\lambda_1 - 1}[2A_{34}A_{41}\rho_1^{\lambda_1} + (A_{34} + A_{41})\rho_2^{\lambda_2} \\
&\quad + (A_{34}B_{41} + A_{41}B_{34})] - \lambda_2 \rho_2^{\lambda_2 - 1}[(A_{41} + A_{34})\rho_1^{\lambda_1} \\
&\quad + 2\rho_2^{\lambda_2} + (B_{41} + B_{34})]]/4 \\
\partial N_2/\partial \eta &= C_2[\lambda_1 \rho_1^{\lambda_1 - 1}[2A_{34}A_{41}\rho_1^{\lambda_1} + (A_{34} + A_{41})\rho_2^{\lambda_2} \\
&\quad + (A_{34}B_{41} + A_{41}B_{34})] + \lambda_2 \rho_2^{\lambda_2 - 1}[(A_{41} + A_{34})\rho_1^{\lambda_1} \\
&\quad + 2\rho_2^{\lambda_2} + (B_{41} + B_{34})]]/4 \\
\partial N_3/\partial \xi &= C_3[\lambda_1 \rho_1^{\lambda_1 - 1}[2A_{41}A_{12}\rho_1^{\lambda_1} + (A_{41} + A_{12})\rho_2^{\lambda_2} \\
&\quad + (A_{41}B_{12} + A_{12}B_{41})] - \lambda_2 \rho_2^{\lambda_2 - 1}[(A_{12} + A_{41})\rho_1^{\lambda_1} \\
&\quad + 2\rho_2^{\lambda_2} + (B_{12} + B_{41})]]/4 \\
\partial N_3/\partial \eta &= C_3[\lambda_1 \rho_1^{\lambda_1 - 1}[2A_{41}A_{12}\rho_1^{\lambda_1} + (A_{41} + A_{12})\rho_2^{\lambda_2} \\
&\quad + (A_{41}B_{12} + A_{12}B_{41})] + \lambda_2 \rho_2^{\lambda_2 - 1}[(A_{12} + A_{41})\rho_1^{\lambda_1} \\
&\quad + 2\rho_2^{\lambda_2} + (B_{12} + B_{41})]]/4 \\
\partial N_4/\partial \xi &= C_4[\lambda_1 \rho_1^{\lambda_1 - 1}[2A_{12}A_{23}\rho_1^{\lambda_1} + (A_{12} + A_{23})\rho_2^{\lambda_2} \\
&\quad + (A_{12}B_{23} + A_{23}B_{12})] - \lambda_2 \rho_2^{\lambda_2 - 1}[(A_{23} + A_{12})\rho_1^{\lambda_1} \\
&\quad + 2\rho_2^{\lambda_2} + (B_{23} + B_{12})]]/4 \\
\partial N_4/\partial \eta &= C_4[\lambda_1 \rho_1^{\lambda_1 - 1}[2A_{12}A_{23}\rho_1^{\lambda_1} + (A_{12} + A_{23})\rho_2^{\lambda_2} \\
&\quad + (A_{12}B_{23} + A_{23}B_{12})] + \lambda_2 \rho_2^{\lambda_2 - 1}[(A_{23} + A_{12})\rho_1^{\lambda_1} \\
&\quad + 2\rho_2^{\lambda_2} + (B_{23} + B_{12})]]/4
\end{aligned} \tag{7}$$

These derivatives clearly show that there are singularities of order $(-1 + \lambda_1)$ and $(-1 + \lambda_2)$ at the points $\rho_1 \to 0$ and $\rho_2 \to 0$ respectively.

EXAMPLES

The TSP element has been incorporated in a 2-D finite element code 'CRACK'.[6] A few case studies are presented below. In all examples a plane stress situation has been assumed.

The first example deals with a branch crack in a long elastic tension strip with details as shown in Figure 2. This problem has also been studied by Tracey and Cook.[3] The tip of the crack has a singularity given by $\lambda_1 = 0{\cdot}5$ and the singularity at the knee is given by $\lambda_2 = 0{\cdot}674$. Tracey and

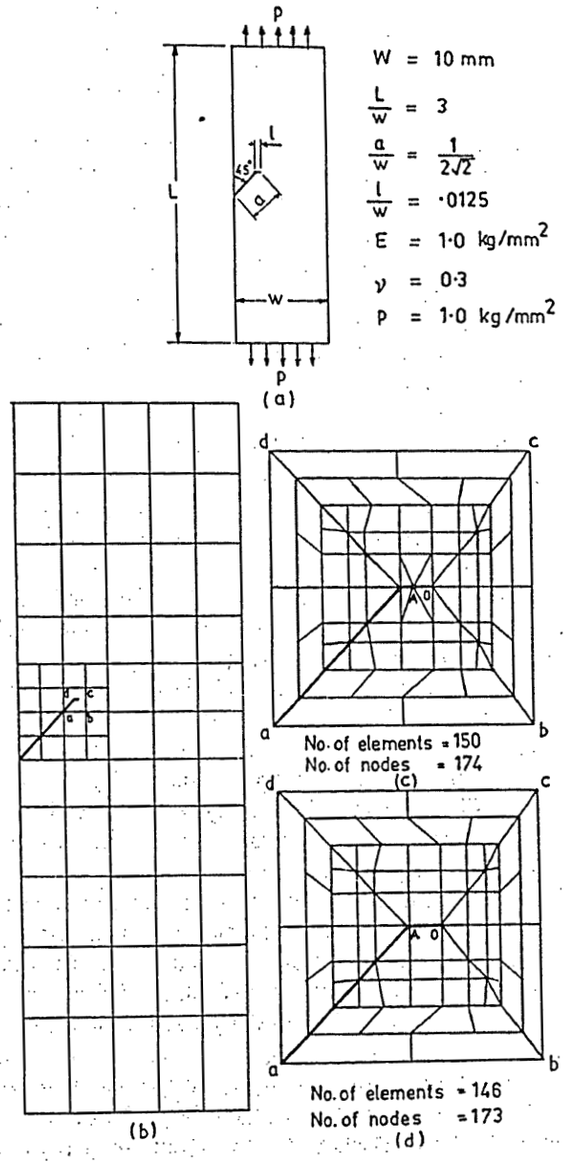

Figure 2. (a) Single edge kinked crack in a long tension strip. (b) Discretization details away from the knee and crack tip. (c) and (d) Two discretization schemes around the knee and crack tip

Table I. Computed mode I SIF for single edge kinked crack in a long tension strip

Tracey and Cook [1977]	Computed SIF (kg mm$^{-3/2}$) using discretization schemes			
	Triangular elements (Figure 2(c))		Rectangular elements (Figure 2(d))	
	Singularities not imposed	Singularities imposed	Singularities not imposed	Singularities imposed (i.e. TSP)
2·317	1·720	2·081	2·068	2·248

Cook[3] have used the 3-noded triangular variable order singularity elements around the crack tip and at the knee to model the two singularities. Apparently ten elements are used in between the knee and the crack tip. The details of discretization and loading are shown in Figure 2. Two discretization schemes were considered. In the first case, only triangular elements were used in between the knee and the crack tip and, in the second case, only one rectangular element was used. Stress intensity factors (SIFs) were calculated based on a direct displacement comparison at A (Figure 2) on the crack face. Computations were done with and without imposition of singularities at the tip of the kink and knee. Mode I SIFs are compared in Table I. The Mode II SIF was found to be of the order of 0·001 kg mm$^{-3/2}$.

The second example considered is shown in Figure 3(a). The order of singularity at the knee changes with the kink angle θ. θ was varied in the range 15° to 90°, in steps of 15°. The values of λ at the knee corresponding to the six kink angles[1] are shown in Table II. The similar problem has been studied earlier in References 5 and 7 using quarter point triangular singularity elements at the crack tip and 6-noded triangular elements around the knee. In all 667 nodes and 210 elements were used in these investigations.[7]

The element arrangements near the crack tip for $\theta = 90°$ and 45° are shown in Figures 3(c) and 3(d) respectively. The far away region is discretized as shown in Figure 3(b). To permit a study of the case $\theta = 75°$, the discretization shown in Figure 3(c) was amended by modifying the relevant nodal co-ordinates. Similarly the discretization shown in Figure 3(d) was modified to accommodate the cases $\theta = 60°$, $\theta = 30°$ and $\theta = 15°$. Most of the elements used were 4-noded quadrilaterals. Few variable noded elements were employed in the transition zones between coarse and fine regions. The J-integral was computed along the three contours lying in the region bounded by the curves c_1 and c_2 as shown in Figures 3(c) and 3(d). It may be noted that, in the presence of the TSP element, a portion of the J contour must lie within this element; the remaining portion can, however, be made to pass through different elements.

The effect of near tip mesh refinement on computed J was studied by considering three different discretizations. To facilitate these three cases a refined element arrangement (Figure 4) is introduced. The first discretization corresponds to a combination of Figures 3(b) and 3(d). The second one corresponds to a combination of Figures 4(a) and 3(d). The third scheme corresponds to a combination of Figures 4(a) and 4(b). For this study θ was considered to vary from 15° to 60° only.

Table III presents results related to the path independence of J and the influence of mesh refinement on J computation. In this table J based on the analytical method[4] is also included. Average J values are compared with the analytical results[4] and computed values of Reference 5 in Table II. The influence of mesh refinement on the crack opening displacement (COD) in the loading direction at the knee is shown in Table IV.

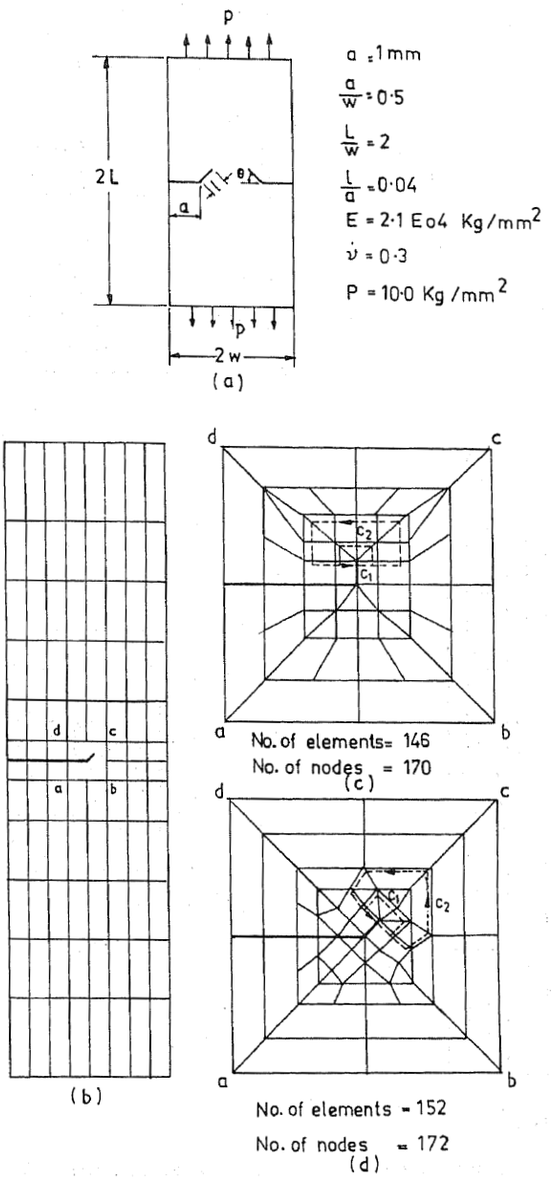

Figure 3. (a) Double edge kinked cracks in a tension strip. (b), (c) and (d) Discretization details

The third example (Figure 5) deals with an asymmetrically branched crack in an infinite plate subjected to uni-directional tensile load. This type of problem has been studied analytically by many investigators.[8-12] Only the case of a 45° branched crack was examined here. For the proportion of the crack shown in Figure 5 the plate can very well be treated as an infinite body. The discretization scheme employed is shown in Figure 5. In this analysis the kink dimension was held constant but the main crack length was varied. The first case was considered with the main

Tabel II. Comparisons of J in the double edge kinked cracks in a tension strip

Kink angle	λ	J (kg mm/mm^2) Analytical (Ref. 4)	Finite element based (Ref. 5)	Present computation	Percentage difference with analytical
15°	0·85733	0·019858	—	0·019476	−1·92
30°	0·75197	0·01789	0·0184	0·017570	−1·77
45°	0·67358	0·01497	0·0151	0·014526	−2·96
60°	0·61573	0·01156	0·0112	0·010900	−5·68
75°	0·57386	0·00814	0·00754	0·007666	−5·82
90°	0·54448	0·005138	—	0·004950	−3·66

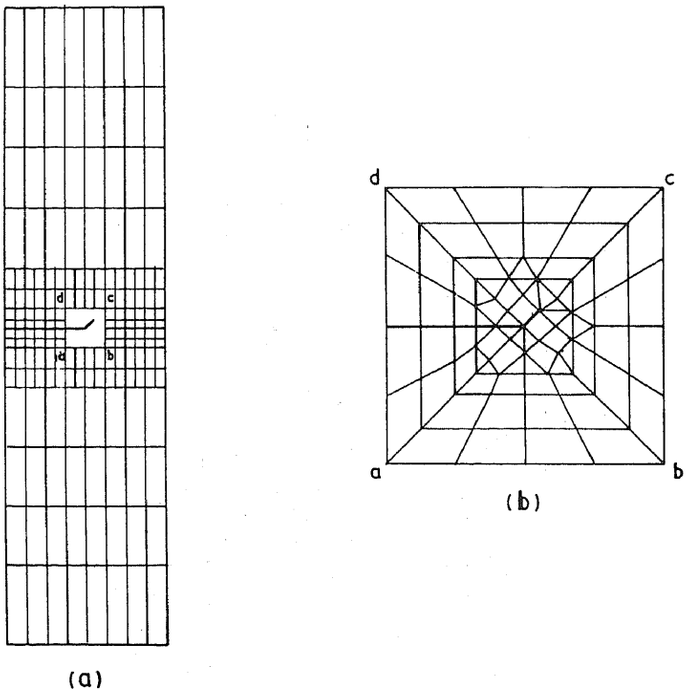

Figure 4. A refined discretization for the double edge kinked crack: (a) discretization away from the kink; (b) discretization near the kink

crack extending from 1 to 9 and the kink extending from 9 to 10 (Figure 5). For the second case the left hand tip of the main crack was shifted from location 1 to 2 and the appropriate pair of nodes lying between 1 and 2 were made to coalesce. Thus seven cases were studied by varying the left hand tip locations from 1 to 7 (Figure 5). The J integral was computed along three different contours. A comparison with the results of Lo[8] is presented in Table V and Figure 6 for different c/l ratios. Lo's results, which are quoted in terms of K_I and K_{II}, were converted in terms of J for this comparison.

Table III. Effect of mesh refinement on J computation in the case of double edge kinked crack problem

		J (kg mm/mm^2)					
		Mesh 1 (No. of elements = 152. No. of nodes = 172)		Mesh 2 (No. of elements = 236. No. of nodes = 275)		Mesh 3 (No. of elements = 256. No. of nodes = 287)	
θ	Analytical (Ref. 4)	Based on three contours	Average	Based on three contours	Average	Based on three contours	Average
15°	0·019858	0·01938 0·01887 0·02018	0·019476	0·01928 0·01875 0·02007	0·019366	0·01946 0·01921 0·02011	0·01959
30°	0·01789	0·01733 0·01720 0·01819	0·01757	0·01721 0·01706 0·01806	0·017443	0·01745 0·01743 0·01812	0·017666
45°	0·01497	0·01430 0·01473 0·01455	0·014526	0·01449 0·01429 0·01473	0·014503	0·01504 0·01489 0·01495	0·01496
60°	0·01156	0·01190 0·01043 0·01038	0·01090	0·01002 0·00996 0·01017	0·01005	0·01076 0·01068 0·01062	0·010686

Table IV. Influence of mesh refinement on crack opening displacement (COD) in the loading direction at the knee

Kink angle θ	COD (mm)		
	Mesh 1	Mesh 2	Mesh 3
15°	0·000616	0·000616	0·000623
30°	0·000580	0·000580	0·000588
45°	0·000540	0·000540	0·000548
60°	0·000486	0·000480	0·000490

DISCUSSION AND CONCLUSIONS

The formulation given above presents a radical approach for modelling arbitrary singularities occurring at two neighbouring points in a domain by a single element. The new element offers a very elegant and computationally advantageous way of modelling a propagating crack that is handled in a step-by-step analysis, short kinked cracks, corrosion cracks, etc. The element formulation is straightforward and can be easily incorporated in a displacement based finite element package. The case studies presented here indicate that the accuracy of results is improved by using the TSP element in the discretization and this is achieved with a great reduction in computational cost.

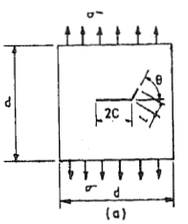

$\theta = 45^\circ$
$d = 20$ mm
$l = 0.4$ mm
$E = 21000$ Kg/mm^2
$\nu = 0.3$
$\sigma = 10$ Kg/mm^2
$0.0875 \leq 2C \leq 1.0$ mm

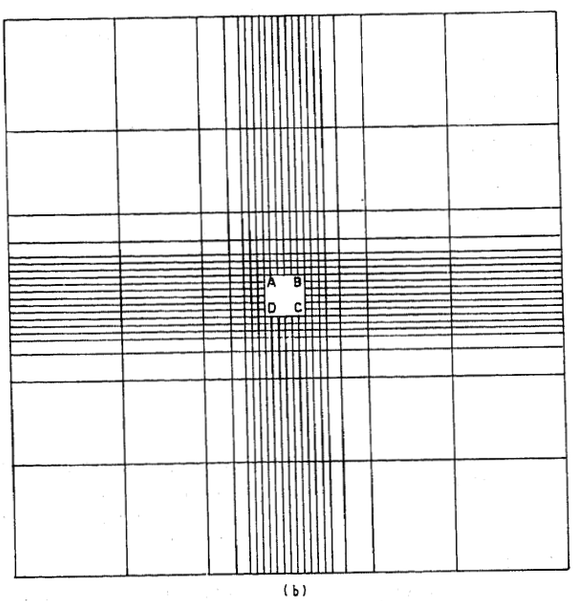

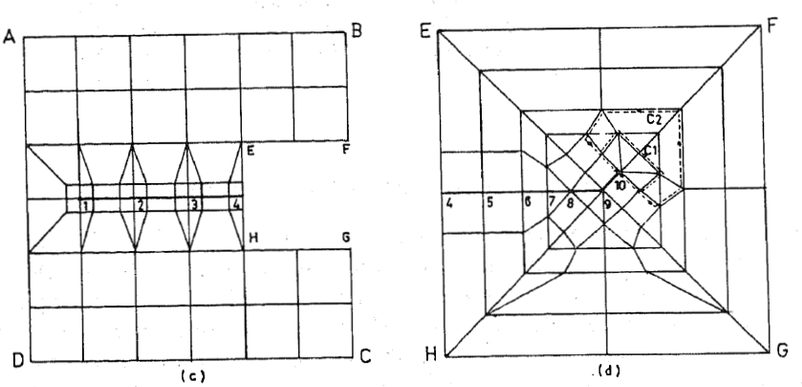

Figure 5. (a) Asymmetrically branched crack in an infinite plate under tension. (b), (c) and (d) Discretization schemes near to and away from the crack

Table V. Comparison of analytical and computed J for the case of asymmetrically branched crack in an infinite plate

c	c/l	Computed J (kg mm/mm^2) Based on different contours	Average	$\frac{EJ_{average}}{\sigma^2 \pi c}$	$\frac{EJ}{\sigma^2 \pi c}$ (Ref. 8)	Percentage difference
0·5	12.5	0·005175 0·005089 0·005263	0·0051756	0·69193	0·68112	+1·58
0·375	9·375	0·003886 0·003825 0·003950	0·0038870	0·69287	0·68731	+0·81
0·25	6·25	0·002618 0·002581 0·002657	0·0026186	0·70018	0·69719	+0·43
0·125	3·125	0·001390 0·001376 0·001404	0·0013900	0·74332	0·74126	+0·28
0·09375	2·34375	0·001103 0·001094 0·001112	0·0011030	0·78645	0·77339	+1·69
0·0625	1·5625	0·0008096 0·0008057 0·0008151	0·0008101	0·86645	0·83969	+3·19
0·04375	1·09375	0·0005968 0·0005962 0·0006014	0·00059813	0·91388	0·92603	−1·31

In the first example, the single edge kinked crack problem, the TSP element helps to obtain better accuracy than the best attainable using the existing singularity elements.[3] In the second example, the double edge kinked crack problem, the computed J values (Table III) are reasonably path independent and are affected marginally by the mesh refinement. We observe that, for $\theta > 60°$, the path independence characteristics of computed J are affected. The difference between the average and the analytical J is less than 6 per cent (Table II). On the whole we are able to obtain an accuracy close to that of Reference 5, in spite of a very low number of nodes (about a fourth) being used in our analysis. There is no reference which could facilitate a comparison of the COD's. However, Tables II, III and IV, can be taken to mean that the displacements have reached a good state of convergence and these can be determined reasonably accurately using a coarse discretization around the crack tip in the presence of a TSP element.

In the third example the computed results are comparable with the analytical solution for the ratios of kink length to half crack length (c/l) varying from 1 (approximately) to 12·5. Therefore the TSP element can be used not only in the case when the kink length is sufficiently small compared with half the main crack length but also for the case when the kink length is comparable to half the main crack length. The TSP element, as it stands, does not meet the completeness requirement. This could lead to difficulties for its adoption in thermal stress problems. Efforts are now being directed to eliminate this shortcoming.

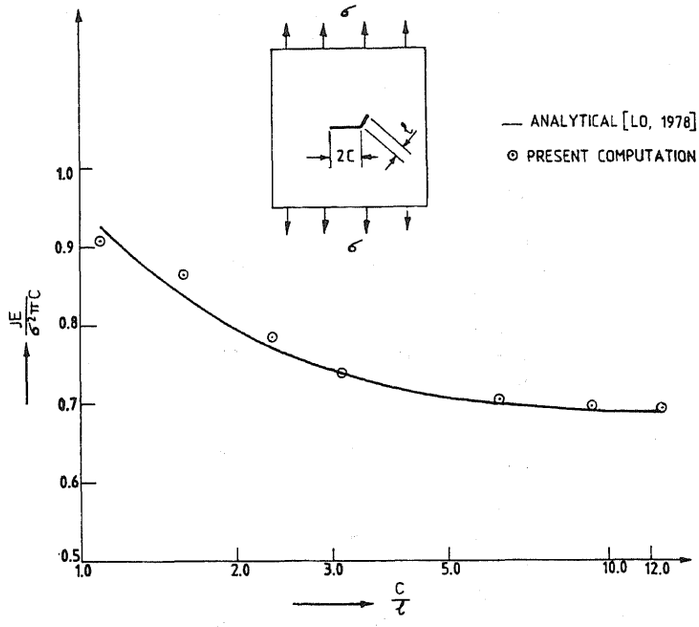

Figure 6. Comparison of analytical and computed J for the case of asymmetrically branched crack in an infinite plate

REFERENCES

1. M. L. Williams, 'Stress singularities resulting from various boundary conditions in angular corners of plates in extension', *J. Appl. Mech. ASME, Series E*, **19**, 526–528 (1952).
2. R. S. Barsoum, 'On the use of isoparametric finite elements in linear fracture mechanics', *Int. j. numer. methods eng.*, **10**, 25–37 (1976).
3. D. M. Tracey and T. S. Cook, 'Analysis of power type singularities using finite elements', *Int. j. numer. methods eng.*, **11**, 1225–1233 (1977).
4. B. Cotterell and J. R. Rice, 'Slightly curved or kinked cracks', *Int. J. Fract.*, **16**, 155–169 (1980).
5. R. Sethuraman and S. K. Maiti, 'Finite element based computation of strain energy release rate by modified crack closure integral', *Eng. Fract. Mech.*, **30**, 227–231 (1988).
6. B. K. Dutta, A. Kakodkar and S. K. Maiti, 'Development of a computer code CRACK for elastic and elastoplastic fracture mechanics analysis of 2-D structure by finite element technique', BARC-1346 (Bhabha Atomic Research Centre, Bombay, India), 1986.
7. S. K. Maiti, 'In-plane fracture toughness of unidirectional fibre composites', *Project No. 391, Final Technical Report*, IIT Bombay, 1987.
8. K. K. Lo, 'Analysis of branched cracks', *J. Appl. Mech.*, **45**, 797–802 (1978).
9. H. Andersson, 'Stress-intensity factors at the tips of a star-shaped contour in an infinite tensile sheet', *J. Appl. Mech.*, **17**, 405–417 (1969).
10. S. N. Chatterjee, 'The stress field in the neighbourhood of a branched crack in an infinite sheet', *Int. J. Solids Struct.*, **11**, 521–538 (1975).
11. B. A. Bilby and G. E. Cardew, 'The crack with a kinked tip', *Int. J. Fract.*, **11**, 708–712 (1975).
12. H. Kitagawa and R. Yuuki, 'Analysis of branched crack under biaxial stresses', *Proc. ICF-4, Vol. 3*, Waterloo, Canada, 1977, pp. 201–211.